Purification and Functional Reconstitution of Soybean Nodulin 26. An Aquaporin with Water and Glycerol Transport Properties†

Robert M. Dean,‡ Ricky L. Rivers,§ Mark L. Zeidel,§ and Daniel M. Roberts*,‡

Department of Biochemistry, Cellular, and Molecular Biology and Center for Legume Research, University of Tennessee, Knoxville, F431 Walters Life Sciences Building, Knoxville, Tennessee 37996, and Laboratory of Epithelial Cell Biology, Renal-Electrolyte Division, University of Pittsburgh Medical Center, 3550 Terrace Street, Pittsburgh, Pennsylvania 15213-2500

Received August 31, 1998; Revised Manuscript Received October 27, 1998

ABSTRACT: Infection of soybean roots by nitrogen-fixing *Bradyrhizobium japonicum* leads to expression of plant nodule-specific genes known as nodulins. Nodulin 26, a member of the major intrinsic protein/aquaporin (AQP) channel family, is a major component of the soybean symbiosome membrane (SM) that encloses the rhizobium bacteroid. To investigate the water and solute transport characteristics of nodulin 26, we purified the protein from SMs and reconstituted it into carboxyfluorescein-loaded liposomes for transport studies using stopped-flow spectrofluorimetry. Liposomes containing nodulin 26 exhibited a high osmotic permeability ($P_f = 0.012 \pm 0.0013$ cm/s), a value fivefold higher than that obtained with control liposomes. Water flux through nodulin 26 showed a low activation energy (E_a) (4.07 kcal/mol) and was reduced 70% upon addition of 1 mM $HgCl_2$. Reconstituted nodulin 26 exhibited a single-channel conductance of $3.8 \pm 2.5 \times 10^{-15}$ cm^3/s ($n = 3$), a value that is lower than other characterized AQPs. Nodulin 26 proteoliposomes also facilitate glycerol transport, showing a 43-fold higher rate of glycerol flux than control liposomes. This observation was supported by expression experiments in *Xenopus* oocytes that showed that nodulin 26 facilitated glycerol flux in a manner indistinguishable from the *Escherichia coli* GlpF glycerol facilitator. Consistent with the results of water transport, glycerol transport was inhibited by $HgCl_2$ and showed a low E_a (4.43 kcal/mol). These results indicate that nodulin 26 is a multifunctional AQP that confers water and glycerol transport to the SM, and likely plays a role in osmoregulation during legume/rhizobia symbioses.

Plants of the Leguminosae family are infected by diazotrophic soil bacteria of the genera *Rhizobium* and *Bradyrhizobium*, leading to the establishment of a nitrogen-fixing symbiosis. During infection, a developmental pathway is triggered that leads to the formation of a novel plant root organ, the nodule (*1*, *2*). During nodule formation the expression of plant-encoded, nodule-specific proteins known as nodulins is induced (*3*; reviewed in refs *1* and *4*). These proteins are proposed to perform functions that are essential for the establishment and maintenance of the symbiosis.

Several nodulins are targeted to the plant-derived symbiosome membrane (SM)[1] (*5*, *6*), which encloses the bacteroid within the symbiotic organelle known as the symbiosome (*7*). The SM serves to protect the bacteroid from plant defense responses and mediates the exchange of metabolites between the plant host and the endosymbiont (*8*). Among the nodulins targeted to the soybean SM is nodulin 26 (*6*, *9*). Nodulin 26 is a major protein component of the SM, constituting approximately 10% of the total membrane protein (*9*, *10*). From the deduced amino acid sequence of nodulin 26 it is clear that it is a member of the major intrinsic protein (MIP) family (*11*, *12*), an ancient membrane protein channel family that includes aquaporin (AQP) water transporters, glycerol transporters, and various other intrinsic membrane proteins (*13*−*17*).

In previous work we have characterized the water and solute transport characteristics of isolated, purified SM vesicles by using a stopped-flow fluorimetric assay (*10*). SM vesicles exhibited a high, facilitated water flux rate that showed low activation energy (E_A), sensitivity to mercurials, and a high P_f/P_d, all characteristics of AQP-mediated water transport (*10*). SM vesicles also showed a mercury-sensitive, facilitated flux of uncharged solutes including glycerol and formamide (*10*). To unequivocally test whether nodulin 26 possesses the water and solute transport activities of the SM, and to rigorously quantify these activities, we have purified and reconstituted native soybean nodulin 26 into liposomes for water and solute flux studies. Further, we have investigated its potential role as a solute transporter upon expression in *Xenopus* oocytes. The results show that nodulin 26 facilitates water and glycerol fluxes at rates that account for the permeability properties of the SM.

† Supported by USDA NRICGP Award 9703548 (D.M.R.) and NIH Grant DK 43955 (M.L.Z.).

* Address correspondence to this author. Phone: 423-974-4070. Fax: 423-974-6306. E-mail: drobert2@utk.edu.

‡ University of Tennessee.

§ University of Pittsburgh.

[1] Abbreviations: AQP, aquaporin; CF, carboxyfluorescein; DTT, dithiothreitol; GlpF, *E. coli* glycerol facilitator; HEPES, *N*-(2-hydroxyethyl)-piperazine-*N*′-ethanesulfonic acid; MIP, major intrinsic protein; MOPS, 3-morpholinopropanesulfonic acid; NMDG, *N*-methyl-D-glucamine chloride; OG, *n*-octyl β-D-glucopyranoside; PIP, plasma membrane intrinsic protein; PMSF, phenylmethylsulfonyl fluoride; SDS-PAGE, sodium dodecyl sulfate−polyacrylamide gel electrophoresis; SM, symbiosome membrane; TIP, tonoplast intrinsic protein.

10.1021/bi982110c CCC: $18.00
Published on Web 12/11/1998

MATERIALS AND METHODS

Purification of Native Nodulin 26 from Soybean Root Nodules. Soybean plants (*Glycine max* cv *Essex*) were infected with *Bradyrhizobium japonicum* and were grown as previously described (*9*, *10*). SMs were isolated from 28- to 35-day-old nodules as described by Weaver and Roberts (*18*). SMs (5−6 mg total protein) were suspended in 20 mL of 7.5 mM sodium phosphate, pH 7.5, 1.0 M KI, 1 mM EDTA, 1 mM dithiothreitol (DTT), 1 μM pepstatin A, 1 mM phenylmethylsulfonyl fluoride (PMSF), and 1 μM leupeptin, and were incubated at 4 °C for 30 min with occasional gentle mixing. The membranes were collected by centrifugation at 100 000*g* for 1 h at 4 °C. The pellet was rinsed with two 5-mL portions of 10 mM Tris-HCl, pH 8.0, was suspended in 10 mL of 10 mM Tris-HCl, pH 8.0, 1 μM pepstatin A, 1 mM PMSF, and 1 μM leupeptin, and was centrifuged at 100 000*g* for 1 h at 4 °C. Nodulin 26 was solubilized in 10 mL of 10 mM Tris-HCl, pH 8.0, 2% (w/v) *n*-octyl β-D-glucopyranoside (OG), 1 μM pepstatin A, 1 mM PMSF, and 1 μM leupeptin and was purified by DEAE Fast Flow chromatography on a Pharmacia FPLC system as previously described (*19*) with the following modifications. After sample application, the column (1.8 mL) was washed with 20 mL of buffer A [10 mM Tris-HCl, pH 8.0, 1% (w/v) OG, 1 μM leupeptin], followed by 20 mL of buffer B [20 mM 2-morpholinoethanesulfonic acid (MES)-NaOH, pH 6.2, 1% (w/v) OG, 1 μM leupeptin]. The column was eluted with a 15-mL linear gradient of 0−0.2 M NaCl, followed by an 8.0-mL linear gradient of 0.2−0.4 M NaCl in buffer B. Fractions containing purified nodulin 26 were concentrated to 0.5−1.0 mg/mL using an Amicon Centricon-10 ultrafiltration device. The sample was dialyzed for 12 h at 4 °C against 100 mL of 20 mM Tris-HCl, pH 7.8, 0.9% (w/v) OG, 0.1 mM 2-mercaptoethanol, and 1 μM leupeptin, and was stored at −80 °C.

Proteoliposome Reconstitution. Proteoliposome reconstitution was done by a rapid dilution protocol as previously described (*20*, *21*). Nodulin 26 (200−250 μg) was combined with 9 mg of bath-sonicated *Escherichia coli* phospholipid (acetone/ether-washed *E. coli* total lipids, Avanti Polar Lipids) in 50 mM Tris-HCl, pH 7.5, and 1.25% (w/v) OG in a final volume of 1.0 mL. Control liposomes were prepared in a similar manner except nodulin 26 was omitted. The mixture was incubated on ice for 30 min, and liposomes were formed by rapidly injecting the sample into 25 mL of 50 mM 3-morpholinopropanesulfonic acid (MOPS), pH 7.5, 150 mM *N*-methyl-D-glucamine chloride (NMDG), 10 mM carboxyfluorescein (CF), 1 mM DTT, and 0.5 mM PMSF at room temperature (22−25 °C). The suspension was incubated for 20 min and the liposomes were collected by centrifugation at 120 000*g* for 1 h at 4 °C. The liposome pellet was washed in 8 mL of 50 mM MOPS, pH 7.5, and 150 mM NMDG and was centrifuged at 120 000*g* for 1 h at 4 °C. The washing step was repeated until CF was no longer detected in the supernatant. The liposome pellet was resuspended in 300 μL of 50 mM MOPS, pH 7.5, and 150 mM NMDG and was stored at 4 °C until analysis.

Membrane Permeability Measurements on Liposomes. Water (P_f) and glycerol ($P_{glycerol}$) permeability coefficients of reconstituted liposomes were determined by using a stopped-flow fluorimetric approach as previously described (*10*, *21*−*24*). Fluorimetry measurements were done with an excitation wavelength of 490 nm with the emission filtered with a 515-nm cutoff filter. Experiments were performed on a Bio-Logic Model SFM-3 with a MPS-51 power supply fitted with a TC-100/10 cuvette, 15-mL syringes, and a HDS mixer, running at a total flow rate of 3 mL/s (80 μL/injection) with a measured dead time of 7 ms. The fluorimeter was controlled by Bio-Kine Software V3.20. Fluorescence data were collected (1000 points) at time intervals of 0.1 ms and 0.5 ms for water permeability measurements and at intervals of 2.0 ms and 10 ms for glycerol permeability measurements. At least 10 individual traces were averaged to reduce the signal-to-noise ratio, and were fitted to a single exponential by using the SigmaPlot software (Jandel Scientific).

Before permeability measurements, anti-CF antibody was added to liposome preparations to quench any residual extravesicular CF fluorescence (*21*−*23*, *25*). Liposomes in 50 mM MOPS, pH 7.5, and 150 mM NMDG (300 mOsm/kg) with entrapped CF (10 mM) were rapidly injected into an identical buffer adjusted to 900 mOsm/kg with sucrose. After mixing, the extravesicular osmolarity (C_{out} = 600 mOsm/kg) was double that of the intravesicular osmolarity (C_{in} = 300 mOsm/kg), resulting in water efflux and the time-dependent quenching of the fluorescence signal as the intravesicular concentration of CF increased. P_f was calculated from the time course of relative fluorescence by comparing single-exponential time constants fitted to simulated curves where P_f was varied as previously described (*10*). Simulated curves were calculated using the MathCad software from the osmotic permeability equation (eq 1).

$$dV(t)/dt = (P_f)(SAV)(MVW)\{[C_{in}/V(t)] - C_{out}\} \quad (1)$$

$V(t)$ is the relative volume of the vesicles at time t, P_f is the osmotic water permeability, SAV is the vesicle surface area-to-volume ratio, MVW is the molar volume of water (18 cm^3/mol), and C_{in} and C_{out} are the total osmolarity inside and outside the liposomes, respectively.

Parameters from the exponential fit (amplitude and endpoint) are used to normalize the fluorescence data using the assumption that the relative volume at $t = 0$ will be 1 and will decrease over time until an equilibrium is reached at a relative volume of 0.5 at the end of the experiment (*21*−*24*).

The single-channel conductance of nodulin 26 was calculated by determining the nodulin 26 content per unit surface area of proteoliposomes by the approach described previously (*21*). The total surface area (SA) of the liposomes was calculated from the SAV calculated from the vesicle diameter and the total internal vesicle volume. The diameter of the liposomes was measured by negative staining with 1% (w/v) uranyl acetate followed by visualization with a transmission electron microscope (Hitachi H-800, 100 kV). The diameters of 30−100 liposomes from each preparation were measured and an average was calculated. The SAV was calculated from the following ratio: $4\pi r^2/(4/3\pi r^3) = 3/r$, where r is the vesicular radius. The total intravesicular volume was determined spectrofluorimetrically as previously described (*10*).

The nodulin 26 concentration was quantified by sodium dodecyul sulfate−polyacrylamide gel electrophoresis of the proteoliposome preparation followed by Coomassie Blue

staining and densitometry (BioRad Model GS-670 Imaging Densitometer). The density value of the nodulin 26 band was compared with a standard curve obtained with purified nodulin 26 standards from the same gel. The unit conductance (pf) was calculated with eq 2.

$$\mathrm{pf} = P_\mathrm{f}/\mathrm{SuD} \quad (2)$$

P_f is the calculated osmotic water permeability in cm/s at 20 °C, and SuD is the number of nodulin 26 molecules/cm^2.

Glycerol permeability of liposomes was determined as previously described (*10*). Liposomes were preincubated in 50 mM MOPS, pH 7.5, 150 mM NMDG, and 0.6 M glycerol (900 mOsm/kg) for 15 min at room temperature (22−25 °C). Samples were then rapidly injected into an isoosmotic buffer consisting of 50 mM MOPS, pH 7.5, 150 mM NMDG, and 600 mM sucrose (an impermeant solute). Thus, after mixing, C_in = 600 mOsm/kg glycerol and 300 mOsm/kg impermeant solute and C_out = 300 mOsm/kg glycerol and 600 mOsm/kg impermeant solute. The permeant test solute effluxes out of the liposomes, driven by the solute concentration gradient, and water follows, leading to liposome shrinkage and CF self-quenching. The equation for determining glycerol flux was derived as described in ref *23* and as shown below for our conditions. The general formula for solute flux across a membrane is given as follows:

$$J_\mathrm{z} = \mathrm{d}z/\mathrm{d}t = (P_\mathrm{z})(\mathrm{SA})(\Delta C) \quad (3)$$

where J_z is the flux of a permeant solute "z", P_z is the permeability coefficient for solute z, SA is the surface area of the vesicle, and ΔC is the concentration gradient across the vesicle membrane. If

$$V_\mathrm{rel} = V_{(t)}/V_\mathrm{o} \quad (4)$$

where V_o is the initial volume of the vesicle and V_rel and $V_{(t)}$ are the relative and absolute volumes, respectively, at time t, then for our conditions of glycerol flux upon mixing:

$$\mathrm{d(glycerol)}/\mathrm{d}t = -900(V_\mathrm{o})(\mathrm{d}V_\mathrm{rel}/\mathrm{d}t) \quad (5)$$

$$\Delta C = 1500 - 1200/V_\mathrm{rel} \quad (6)$$

From this the following equation was derived and used to calculate glycerol permeabilities (P_glycerol) using the parameter from the single-exponential fit and the MathCad program.

$$\mathrm{d}V_\mathrm{rel}/\mathrm{d}t = P_\mathrm{glycerol}(\mathrm{SA}/V_\mathrm{o})(1/900)(1200/V_\mathrm{rel} - 1500) \quad (7)$$

Glycerol Permeability Measurements in Xenopus *Oocytes.* The coding regions for nodulin 26 (*10*), *glp*F (*26*; a kind gift of Dr. Christophe Maurel, CNRS, Gif-sur-Yvette, France), and AQP1 (*27*; obtained from the American Type Culture Collection) were cloned into the pXβG-ev1 expression plasmid (*27*). Capped cRNA was prepared by in vitro transcription of each construct, and was injected (40 to 50 ng cRNA/oocyte) into defolliculated, stage VI *Xenopus laevis* oocytes as previously described (*10*). Oocytes were cultured for 72 h at 16 °C in Ringer's solution (96 mM NaCl, 2 mM KCl, 5 mM $MgCl_2$, 600 μM $CaCl_2$, 5 mM *N*-(2-hydroxyethyl)piperazine-*N*′-ethanesulfonic acid (HEPES)-NaOH, pH7.6, 100 ug/mL penicillin-streptomycin, 205 mOsm/kg). The culture medium was changed daily.

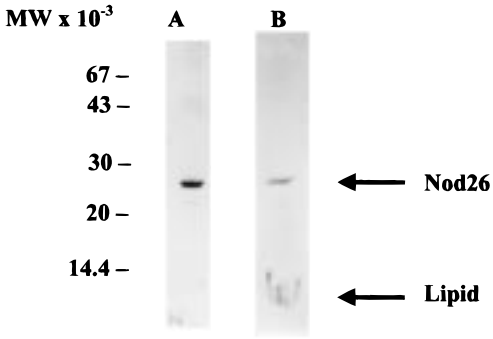

FIGURE 1: Purification and reconstitution of nodulin 26 (Nod26) into liposomes. Nodulin 26 was purified from soybean SMs and was reconstituted into liposomes as described in Materials and Methods. Samples were resolved by SDS-PAGE on a 15% (w/v) polyacrylamide gel and were visualized by Coomassie Blue staining. (Panel A) 3 μg of purified nodulin 26; (panel B) nodulin 26 proteoliposomes, 1 μg protein.

Glycerol uptake experiments were done by a modification of an isotopic glycerol uptake assay (*28*). Oocytes were incubated in borosilicate culture tubes in assay medium (20 μL/oocyte). Assay medium contained 2 mM KCl, 5 mM $MgCl_2$, 600 μM $CaCl_2$, 5 mM HEPES-NaOH pH 7.6, 60 μCi/mL ^{3}H-glycerol (80 Ci/mmol, NEN, Boston, MA), and various concentrations of unlabeled glycerol. The osmolarity of the assay medium was adjusted with NaCl to maintain isoosmotic conditions (205−215 mOsm/kg). Standard assays were carried out at 20 °C for 10 min. Oocytes were lysed overnight in 2% (w/v) SDS at room temperature and isotopic uptake was determined by liquid scintillation counting.

For E_a measurements, assay temperatures were varied between 10 °C to 30 °C. For mercury inhibition experiments, oocytes were preincubated in Ringer's solution containing 1 mM $HgCl_2$ (200 μL/oocyte) for 10 min at 22 °C. The sample was rinsed gently with 2 mL of Ringer's solution (200 μL/oocyte) and the standard uptake assay was performed. To test reversibility, the mercury-treated oocytes were incubated with 2 mL of Ringer's solution with 10 mM 2-mercaptoethanol for 10 min before assay.

General Analytical Methods. Protein concentrations were determined using the BCA method (Pierce Biochemicals) with bovine serum albumin used as a protein standard. SDS−polyacrylamide gel electrophoresis (PAGE) was performed by the method of Laemmli (*29*) on 15% (w/v) polyacrylamide gels. Osmolarities of all solutions were determined by freezing-point depression by using an Osmette A Osmometer (Precision Instruments).

RESULTS

Purification and Reconstitution of Nodulin 26 into Liposomes. Nodulin 26 was solubilized from soybean SMs and was purified to homogeneity by FPLC on DEAE-Fast Flow (Figure 1A). The protein was reconstituted in liposomes by rapid dilution of the purified protein/octylglucoside mixture into *E. coli* phospholipids. Control liposomes were made in a simlar fashion except protein was omitted. After ultracentrifugation, the lipid pellet was examined by uranyl acetate negative staining and visualization using transmission electron microscopy. Both control and nodulin 26 liposomes (Table 1) were present as a uniform population of approximately the same average diameter (119 ± 31 nm for

Table 1: Summary of Water and Glycerol Permeability Values of Nodulin 26 Proteoliposomes, Control Liposomes, and SM Vesicles

	nodulin 26 proteoliposomes	control liposomes	SM vesicles[a]
diameter (nm)	119 ± 31 ($n = 4$)[b]	111 ± 23 ($n = 3$)	228
P_f cm/s (20 °C)	0.012 ± 0.0013 ($n = 5$)	0.0028 ± 0.001 ($n = 5$)	0.05
P_f cm/s (20 °C) w/$HgCl_2$	0.0036 ± 0.0008 ($n = 4$)		0.0038
unit cond. (pf, cm^3/s), 20 °C	$3.8 \pm 2.5 \times 10^{-15}$ ($n = 3$)		3.2×10^{-15}
E_a (kcal/mol)	4.07 ± 1.53 ($n = 4$)	14.8 ± 3.4 ($n = 4$)	3.3
$P_{gly} \times 10^{-5}$ cm/s (20 °C)	0.87 ± 0.32 ($n = 3$)	0.020 ± 0.007 ($n = 3$)	3.2
$P_{gly} \times 10^{-5}$ cm/s (20 °C) with $HgCl_2$	0.058 ± 0.025 ($n = 3$)		0.5
P_f/P_{gly}	1380		1560

[a] Data from ref *10*. [b] ±SD.

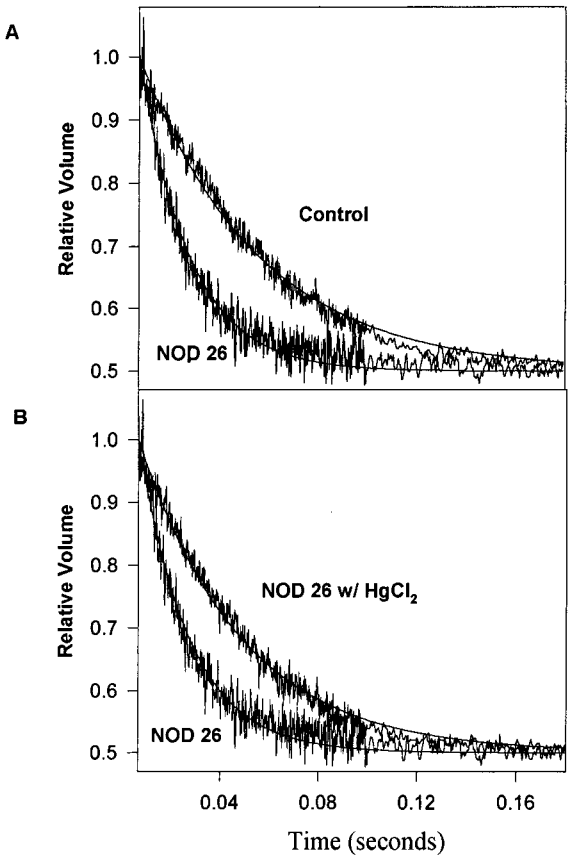

FIGURE 2: Time course of water efflux from nodulin 26 proteoliposomes and control liposomes. Water efflux from CF-loaded liposomes was monitored at 20 °C as the time course of CF self-quenching. Shown are representative average traces of (A) nodulin 26 proteoliposomes and control liposomes and (B) nodulin 26 proteoliposomes both in the presence and absence of 1.0 mM $HgCl_2$. The fit of the data to a single exponential is shown.

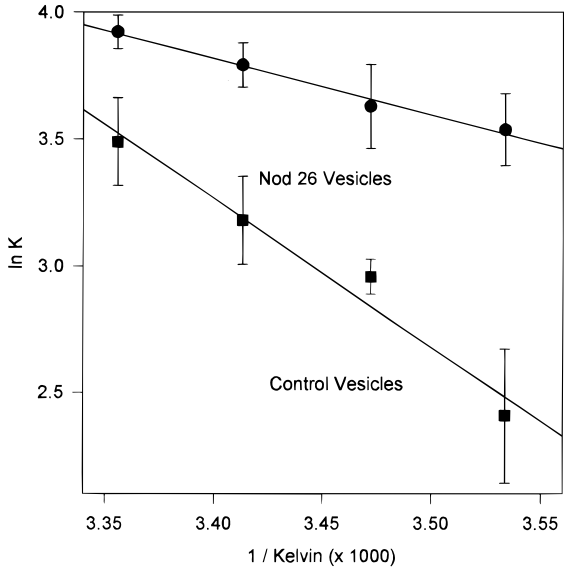

FIGURE 3: Arrhenius plots of water efflux from nodulin 26 proteoliposomes and control liposomes. Arrhenius E_a plots for nodulin 26 proteoliposomes (●) and pure lipid control liposomes (■) are shown. ln K represents the natural log of the rate constant determined from the single-exponential fit of the permeability data similar to that shown in Figure 2. The inverse of temperature (10, 15, 20, and 25 °C) is plotted as degrees kelvin (×1000). Values are the average of three determinations with error bars showing the S. D.

nodulin 26 liposomes and 111 ± 23 nm for control liposomes). Further, SDS−PAGE of the liposome preparation (Figure 1B) verified the presence of nodulin 26 and allowed quantification of the nodulin 26 content for the single channel measurements listed below.

Osmotic Water Permeability of Nodulin 26 Liposomes. The P_f of CF-loaded liposomes was measured after rapidly doubling the extravesicular osmolarity by using stopped-flow fluorimetry (Figure 2). Nodulin 26 proteoliposomes ($P_f = 0.012 \pm 0.0013$ cm/s, $n = 5$) show a four- to fivefold greater rate of water efflux than control liposomes ($P_f = 0.0028 \pm 0.001$ cm/s, $n = 5$) (Figure 2A). Further, consistent with several other AQPs, the flux of water from nodulin 26 proteoliposomes was substantially inhibited ($P_f = 0.0036 \pm 0.0008$ cm/s, $n = 4$) by incubation with 1 mM $HgCl_2$ (Figure 2B). Nodulin 26 possesses two cysteine residues, C55 and C172 (*6*, *11*), within the first and fourth putative transmembrane regions, and presumably Hg^{2+} inhibition results from the modification of either or both of these residues.

Examination of the water permeability of nodulin 26 proteoliposomes as a function of temperature was determined, and the E_a was calculated from Arrhenius plots (Figure 3). Nodulin 26 proteoliposomes transport water with a low E_a (4.07 kcal/mol) compared with that of control liposomes (14.8 kcal/mol). A high rate of water transport, mercurial sensitivity, and a low E_a for the proteoliposomes show that nodulin 26 is facilitating water flux as an AQP.

A measure of the intrinsic flux of water through an AQP is provided by determining its single-channel conductance (pf). This value is an estimation of the amount of water each nodulin 26 channel can transport per unit time with the assumption that, similar to AQP1 (*30*), each nodulin 26 subunit contains one aqueous pore. From the concentration of nodulin 26 monomer within the proteoliposomes (which averaged approximately 3 μM) and the unit surface area of the proteoliposome preparation, a unit conductance of 3.8 $\pm$ 2.5 $\times$ 10^{-15} cm^3/s ($n = 3$) was determined. From water permeability measurements of isolated SM vesicles and the

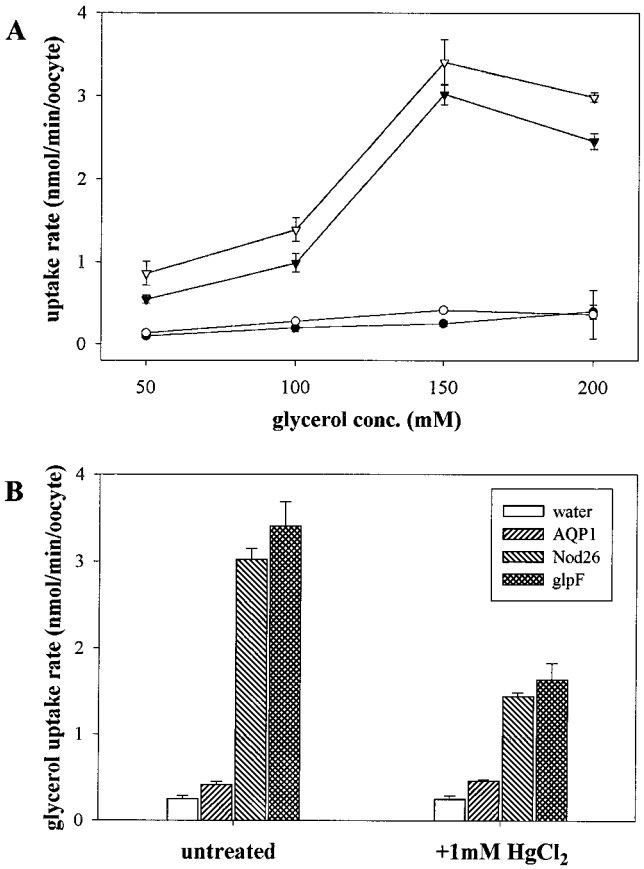

FIGURE 4: Glycerol uptake in *Xenopus* oocytes expressing nodulin 26. cRNA from nodulin 26, GlpF, and AQP1 or a sterile water control were microinjected into *Xenopus* oocytes and ^{3}H-glycerol uptake was performed as described in the Materials and Methods. (A) Concentration-dependent uptake of glycerol by oocytes injected with sterile water (●) or cRNAs encoding nodulin 26 (▼), GlpF (▽), or AQP1 (○). (B) Effects of preincubation of oocytes with 1 mM $HgCl_2$ before glycerol transport analysis. The values represent the average of four to six determinations ± S. E.

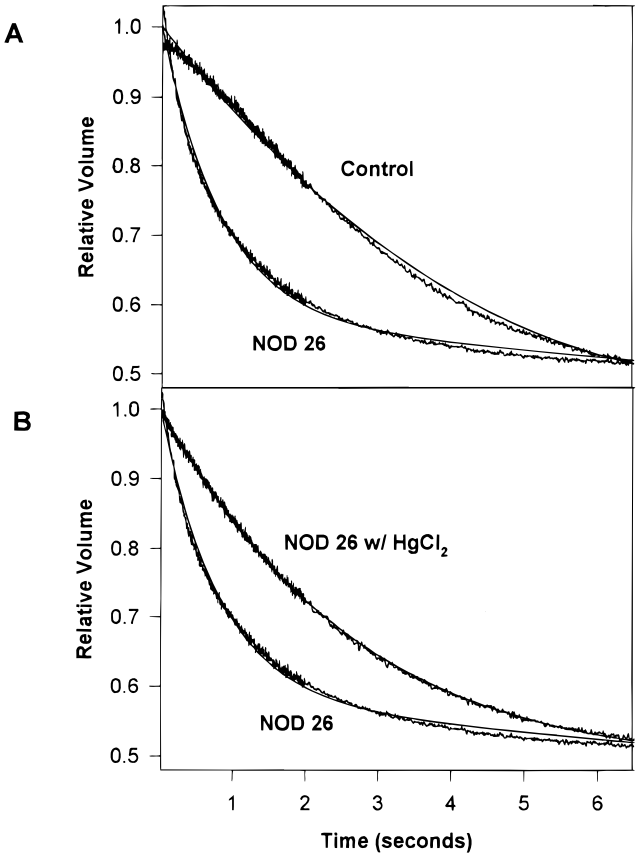

FIGURE 5: Time course of glycerol efflux from nodulin 26 proteoliposomes and control liposomes. Glycerol efflux from CF-loaded liposomes was monitored at 20 °C as the time course of CF self-quenching as described in Materials and Methods. Shown are representative average traces of (A) nodulin 26 proteoliposomes and control liposomes; (B) nodulin 26 proteoliposomes in the presence or absence of 1.0 mM $HgCl_2$. The fit of the data to a single exponential is shown.

endogenous concentration of nodulin 26 on this membrane, a single-channel conductance of 3.2×10^{-15} cm^3/s is predicted (Table 1). The findings show that the water transport properties of nodulin 26 are sufficient to account for the facilitated water transport observed across the SM.

Glycerol Permeability of the Nodulin 26 Channel. To test whether nodulin 26 possesses solute as well as water transport capabilities, its glycerol transport capabilities were investigated in *Xenopus* oocytes as well as in the reconstituted proteoliposomes. *Xenopus* oocytes expressing nodulin 26 showed a concentration-dependent glycerol uptake activity that is comparable with uptake rates observed in oocytes expressing the *E. coli* glycerol facilitator GlpF (Figure 4). The peak uptake rate observed by nodulin 26-expressing oocytes is 12-fold over negative control oocytes injected with sterile water or oocytes expressing the water-specific AQP1 (Figure 4). Preincubation of both GlpF and nodulin 26 oocytes with 1 mM $HgCl_2$ resulted in 50% inhibition of glycerol transport activity (Figure 4B), which was reversible by transfer of oocytes to 2-mercaptoethanol (data not shown). Mercury showed no effect on glycerol transport in negative control oocytes (Figure 4B). Further, calculation of E_a from Arrhenius plots indicates that glycerol transport by oocytes expressing GlpF ($E_a = 3.61$ kcal/mol) and nodulin 26 ($E_a =$ 4.43 kcal/mol) is facilitated, whereas negative control oocytes possessed a high E_a (11.8 kcal/mol) characteristic of diffusion through a lipid bilayer.

Further evidence that nodulin 26 can facilitate glycerol flux was obtained with proteoliposomes by using the stopped-flow fluorimetric method (Figure 5). Glycerol efflux from nodulin 26 proteoliposomes was rapid, showing a 43-fold higher rate ($P_{glycerol} = 0.868 \pm 0.322 \times 10^{-5}$ cm/s, $n = 3$ at 20 °C) than negative control pure lipid liposomes ($P_{glycerol} = 0.020 \pm 0.007 \times 10^{-5}$ cm/s, $n = 3$), (Figure 5A). Similar to the results with oocytes, glycerol transport in nodulin 26 proteoliposomes was inhibited by incubation with 1 mM $HgCl_2$ ($P_{glycerol} = 0.058 \pm 0.025 \times 10^{-5}$ cm/s, $n = 3$), (Figure 5B). Although nodulin 26 proteoliposomes show a high glycerol flux, the smaller solute urea was not transported (data not shown). This explains the poor permeability of the SM to urea (*10*), and suggests a pore selectivity of nodulin 26 for the type of solute transported that is independent of size.

DISCUSSION

Nodulin 26 reconstituted into liposomes facilitates water flux in a $HgCl_2$-sensitive manner with a low E_a and with a single-channel conductance that accounts for the P_f of SMs (Table 1). Additionally, nodulin 26 is multifunctional and also facilitates the transport of glycerol at a rate that accounts

for the permeability of the SM to this solute (Table 1). Thus, the present study establishes nodulin 26 as a unique AQP that is specifically expressed in nodules, and is targeted to the SM, where it confers a high permeability to water and uncharged solutes such as glycerol.

Nodulin 26 As An Aquaglyceroporin. Although AQPs are a structurally and functionally homologous class of proteins, it is becoming clear that differences exist between their intrinsic water transport rates and transport selectivities. Analysis of various mammalian AQPs by functional reconstitution of purified proteins (*21*) or upon expression in *Xenopus* oocytes (*31*, *32*) show a range of single-channel conductance values, with lens MIP (AQP0) showing a water transport activity at least one order of magnitude less than the other AQPs (*31*−*34*). The present study shows that, similar to MIP (AQP0), nodulin 26 shows a low single-channel conductance that is 10- to 50-fold lower than AQP1−5 (*31*−*34*). These differences in intrinsic water transport rates are intriguing, and suggest that one reason for the diversity of AQP isotypes may be to control the rate of water flux by the type of AQP inserted in a membrane. The structural differences that account for these differences in intrinsic transport activity remain unknown. On the basis of comparisons of P_f/P_d ratios, the length of the nodulin 26 channel is proposed to be longer than that of AQP1 (*10*). Structural analyses of nodulin 26, and comparison with the well-characterized AQP1 structure (*35*, *36*) might provide clues to differences that could account for this functional disparity.

The present study shows that nodulin 26 also transports glycerol. Glycerol transport has been reported for selected MIP family members such as the bacterial glycerol facilitator GlpF (*26*, *28*, *37*), mammalian AQP3 (*32*, *38*−*40*) and AQP7 (*41*), and the yeast FPS1 protein (*42*). These proteins represent a functional subclass, referred to as aquaglyceroporins (*17*), that possess the ability to transport uncharged solutes. However, even among these proteins, there are functional distinctions. For example, whereas the GlpF is selective for glycerol (*26*), AQP3 and 7 and nodulin 26 transport both water and glycerol. Further, nodulin 26 is distinct from AQP3 (*32*, *38*) because it has a lower single-channel conductance, and does not flux urea. These findings further underscore the functional diversity of this membrane protein family, and the complexity of AQP pore selectivity.

MIPs are widely distributed in plants, and several have been shown to have AQP activities (reviewed in ref *16*). In a recent study, the plant MIP gene family was characteized in *Arabidopsis* and 23 members were identified (*43*). Gene products were catagorized into three classes, the plasma membrane AQP (PIPs), the tonoplast membrane AQPs (TIPs), and a third, smaller category containing the AQP At−NLM 1. Nodulin 26 appears to be part of this third group (*43*). Interestingly, TIP and PIP proteins show a high selectivity for water and do not exhibit any detectable flux of glycerol (*26*, *44*, *45*). Thus, nodulin 26 is the first plant AQP to be shown to have both water and glycerol transport activities. It will be interesting to investigate other members of the nodulin 26/At−NLM 1 subclass to determine whether this functional property is shared. Also, single-channel measurements of various plant AQPs should be investigated to determine whether, similar to their mammalian counterparts, a range of water transport rates occur. This is especially important because the P_f values of different plant membranes vary over a range of three orders of magnitude (*16*).

Function of Nodulin 26 in the Symbiosome. Because nodulin 26 is among the nodulins that are targeted to the SM (*5*, *6*), a transport role that supports the rhizobia−legume symbiosis has been argued. The SM mediates the metabolite exchange process, which is the crux of the symbiosis: the transport of dicarboxylates into the symbiosome for utilization by the rhizobia bacteroids, and the efflux of fixed ammonium ions for assimilation by the plant (*8*). A role for nodulin 26 as an ion-conducting pore that might facilitate the flux of dicarboxylates was proposed on the basis of reconstitution experiments in planar lipid bilayers (*19*) and similarities to MIP (*46*). Further, an increased rate of malate transport across the SM that is correlated with the in vitro phosphorylation of nodulin 26 has been observed (*47*). However, neither MIP (*33*, *34*) nor nodulin 26 (Chandy, Roberts, and Hall, unpublished) shows ion conductance upon expression in *Xenopus*, and it remains uncertain whether this activity occurs in vivo.

In contrast, the data from native SM vesicles (*10*), nodulin 26-expressing oocytes, and reconstituted proteoliposomes provide compelling evidence that nodulin 26 fluxes water and uncharged solutes. Thus, a potential osmoregulatory role for nodulin 26 can be proposed. For example, as ions and metabolites cross the SM (generating an osmotic gradient), rapid facilitated water flow through nodulin 26 would mediate an osmotic adjustment to maintain an equilibrium between the symbiosome space and the plant cell cytosol. In addition, the regulation of osmotic pressure gradients across the SM could affect the growth and physiology of the bacteroid (*48*).

Additionally, symbiosomes occupy a considerable amount of the intracellular space of the infected cell (*8*). Thus, similar to models of the vacuole in osmoregulation in other plant cells (*16*), the reversible uptake and efflux of water from the symbiosome could contribute to control of the volume of the infected cell, as well as cytosol volume homeostasis and the extracellular space. Finally, several plant AQPs are regulated by osmotic stresses such as drought and high salinity (*43*, *49*, *50*; reviewed in refs *16* and *44*), suggesting that the control of these proteins may help adaptation to conditions of water limitation. Nodules also show a high sensitivity to osmotic stress (*51*), and the modulation of the expression or activity of nodulin 26 could affect water relations within the infected cell during stress.

The glycerol transport activity of nodulin 26 argues that it functions as more than an AQP on the SM. Glycerol transport by AQP analogues has been implicated in metabolic as well as osmoregulatory roles. For example, the bacterial GlpF protein aids in the uptake and utilization of glycerol (*28*, *37*, *52*). On the other hand, glycerol is accumulated as an osmolyte in yeast, fungi, algae, and certain higher plant species where it serves as an osmoprotectant (*53*−*55*) or as a mechanism for turgor generation (*56*). The FPS1 protein of yeast facilitates glycerol transport, and genetic analyses show that it plays an essential osmoregulatory role in the uptake or release of this solute (*42*, *57*). Nodules, like other plant tissues, accumulate osmoprotectant compounds in response to osmotic stresses (*58*). However, whether glycerol is among the compatible solutes accumulated in nodules, and

whether nodulin 26 has a role in the transport of these, remains to be determined.

ACKNOWLEDGMENT

We thank James Guenther, The University of Tennessee, Knoxville, for assisting in electron microscopic measurements of liposomes. We also thank Dr. Peter Gresshoff, The University of Tennessee, Knoxville, for providing greenhouse space for the cultivation of soybeans. We also thank Burnette Crombie for her excellent technical assistance.

REFERENCES

1. Mylona, P., Pawlowski, K., and Bisseling, T. (1995) *Plant Cell 7*, 869−885.
2. Long, S. R. (1996) *Plant Cell 8*, 1885−1898.
3. Legocki, R. P., and Verma, D. P. S. (1980) *Cell 20*, 153−163.
4. Franssen, H. J., Nap, J. P., and Bisseling, T. (1992) in *Biological Nitrogen Fixation* (Stacey, G., Burris, R. H., and Evans, H. J., Eds.) pp 349−398, Chapman and Hall, New York.
5. Fortin, M. G., Zelechowska, M., and Verma, D. P. S. (1985) *EMBO J. 4*, 3041−3046.
6. Fortin, M. G., Morrison, N. A., and Verma, D. P. S. (1987) *Nucleic Acids Res. 15*, 813−824.
7. Roth, E., Jeon, K., and Stacey, G. (1988) in *Molecular Genetics of Plant Microbe Interactions* (Palcios, R., and Verma, D. P. S., Eds.) pp 220−225, ADS Press, St. Paul, MN.
8. Udvardi, M. K., and Day, D. A. (1997) *Annu. Rev. Plant Physiol. Plant Mol. Biol. 48*, 493−523.
9. Weaver, C. D., Crombie, B., Stacey, G., and Roberts, D. M. (1991) *Plant Physiol. 95*, 222−227.
10. Rivers, R. L., Dean, R. M., Chandy, G., Hall, J. E., Roberts, D. M., and Zeidel, M. L. (1997) *J. Biol. Chem. 272*, 16256−16261.
11. Sandal, N. N., and Marcker, K. A. (1988) *Nucleic Acids Res. 16*, 9347.
12. Shiels, A., Kent, N. A., McHale, M., and Bangham, J. A. (1988) *Nucleic Acids Res. 16*, 9348.
13. Chrispeels, M. J., and Agre, P. (1994) *Trends Biochem. Sci. 19*, 421−425.
14. King, L. S., and Agre, P. (1996) *Annu. Rev. Physiol. 58*, 619−648.
15. Park, J. H., and Saier, M. H., Jr. (1996) *J. Membr. Biol. 153*, 171−180.
16. Maurel, C. (1997) *Annu. Rev. Plant Physiol. Plant Mol. Biol. 48*, 399−429.
17. Agre, P., Bonhivers, M., and Borgnia, M. J. (1998) *J. Biol. Chem. 273*, 14659−14662.
18. Weaver, C. D., and Roberts, D. M. (1992) *Biochemistry 31*, 8954−8959.
19. Weaver, C. D., Shomer, N. H., Louis, C. F., and Roberts, D. M. (1994) *J. Biol. Chem. 269*, 17858−17862.
20. Kasahara, M., and Hinkle, P. C. (1977) *J. Biol. Chem. 252*, 7384−7390.
21. Zeidel, M. L., Ambudkar, S. V., Smith, B. A., and Agre, P. (1992) *Biochemistry 31*, 7436−7440.
22. Zeidel, M. L., Nielson, S., Smith, B. L., Ambudkar, S. V., Maunsbach, A. B., and Agre, P. (1994) *Biochemistry 33*, 1606−1615.
23. Lande, M. B., Donovan, J. M., and Zeidel, M. L. (1995) *J. Gen. Physiol. 106*, 67−84.
24. Negrette, H., Rivers, R., Gough, A. H., Colombini, M., and Zeidel, M. L. (1996) *J. Biol. Chem. 271*, 11627−11630.
25. Kuypers, F. A., Roelofsen, B., Berendsen, W., Op Den Kamp, J. A. F., and Van Deenen, L. L. M. (1984) *J. Cell Biol. 99*, 2260−2267.
26. Maurel, C., Reizer, J., Schroeder, J. I., and Chrispeels, M. J. (1993) *EMBO J. 12*, 2241−2247.
27. Preston, G. M., Carroll, T. P., Guggino, W. B., and Agre, P. (1992) *Science 256*, 385−387.
28. Maurel, C., Reizer, J., Schroeder, J. I., Chrispeels, M. J., and Saier, M. H., Jr. (1994) *J. Biol. Chem. 269*, 11869−11872.
29. Laemmli, U.K. (1970) *Nature 227*, 680−685.
30. Jung, J. S., Preston, G. M., Smith, B. L., Guggino, W. B., and Agre, P. (1994) *J. Biol. Chem. 269*, 14648−14654.
31. Zampighi, G. A., Kreman, M., Boorer, K. J., Loo, D. D. F., Benzanilla, F., Chandy, G., Hall, J. E., and Wright, E. M. (1995) *J. Membr. Biol. 148*, 65−78.
32. Yang, B., and Verkman, A. S. (1997) *J. Biol. Chem. 272*, 16140−16146.
33. Mulders, S. M., Preston, G. M., Deen, P. M. T., Guggino, W. B., van Os, C. H., and Agre, P. (1995) *J. Biol. Chem. 270*, 9010−9016.
34. Chandy, G., Zamphighi, G. A., Kreman, M., and Hall, J. E. (1997) *J. Membr. Biol. 159*, 24−39.
35. Cheng, A., van Hoek, A. N., Yeager, M., Verkman, A. S., and Mitra, A. K. (1997) *Nature 387*, 627−630.
36. Walz, T., Hirai, T., Murata, K., Heymann, J. B., Mitsuoka, K., Fujiyoshi, Y., Smith, B. L., Agre, P., and Engel, A. (1997) *Nature 387*, 624−627.
37. Heller, K. B., Lin, E. C. C., and Wilson, T. H. (1980) *J. Bacteriol. 144*, 274−278.
38. Ishibashi, K., Sasaki, S., Fushimi, K., Uchida, S., Kuwahara, M., Saito, H., Furukawa, T., Nakajima, K., Yamaguchi, Y., Gojobori, T., and Marumo, F. (1994) *Proc. Natl. Acad. Sci. U.S.A. 91*, 6269−6273.
39. Echevarria, M., Erich, W. E., and Frindt, G. (1996) *J. Biol. Chem. 271*, 25079−25082.
40. Ishibashi, K., Sasaki, S., Fushimi, K., Yamamoto, T., Kuwahara, M., and Marumo, F. (1997) *Am. J. Physiol. 272*, F325−F241.
41. Ishibashi, K., Kuwahara, M., Gu, Y., Y., Kageyama, Y., Tohasaka, A., Suzuki, F., Marumo, F., and Sasaki, S. (1997) *J. Biol. Chem. 272*, 20782−20786.
42. Luyten, K., Albertyn, J., Skibbe, W. F., Prior, B. A., Ramos, J., Thevelein, J. M., and Hohmann (1995) *EMBO J. 14*, 1360−1371.
43. Weig, A., Deswarte, C., and Chrispeels, M. J. (1997) *Plant Physiol. 114*, 1347−1357.
44. Schäffner, A. R. (1998) *Planta 204*, 131−139.
45. Maurel, C., Kado, R. T., Guern, J., and Chrispeels, M. J. (1995) *EMBO J. 14*, 3028−3035.
46. Ehring, G. R., Zampighi, G. A., Horwitz, J., Bok, D., and Hall, J. E. (1990*) J. Gen. Physiol. 96*, 631−664.
47. Ouyang, L.-J., Whelan, J., Weaver, C. D., Roberts, D. M., and Day, D. A. (1991) *FEBS Lett. 293*, 188−190.
48. Gresshoff, P. M., and Rolfe, B. G. (1978) *Planta 142*, 329−333.
49. Yamaguchi-Shinozaki, K., Koizumi, M., Urao, S., and Shinozaki, K. (1992) *Plant Cell Physiol. 33*, 217−224.
50. Yamada, S., Katsuhara, M., Kelly, W. B., Michalowski, C. B., and Bohnert, H. J. (1995) *Plant Cell 7*, 1129−1142.
51. Hunt, S., and Layzell, D. B (1993) *Annu. Rev. Plant Physiol. Mol. Biol. 44*, 483−511.
52. Sweet, G., Gandor, C., Voegele, R., Beuerle, J., Truniger, V., Lin, E. C. C., and Boos, W. (1990) *J. Bacteriol. 172*, 424−430.
53. Goldstein, G., and Nobel, P. S. (1991) *Plant Physiol. 97*, 954−961.
54. Blomberg, A, and Adler, L. (1992) *Adv. Microbiol. Physiol. 33*, 145−212.
55. Cowan, A. K., Rose, P. D., and Horne, L. G. (1992) *J. Exp. Bot. 43*, 1535−1547.
56. de Jong, J. K., McCormack, B. J., Smirnoff, N., and Talbot, N. J. (1997) *Nature 389*, 244−245.
57. Phillips, J., and Herskowitz, I. (1997) *J. Cell Biol. 138*, 961−974.
58. Hu, C. A., Delauney, A. J., and Verma, D. P. S. (1992) *Proc. Natl. Acad. Sci. U.S.A. 89*, 9354−9358.

BI982110C